The influence of the pyrolysis temperature on the catalytic performance of Cobalt and Nickel containing precursor derived ceramics for CO_2 methanation and Fischer-Tropsch synthesis

Miriam Schubert[a], Michaela Wilhelm[b,e], Sebastian Bragulla[b], Chenghao Sun[c], Sarah Neumann[a], Thorsten M. Gesing[d,e], Peter Pfeifer[c], Kurosch Rezwan[b,e], Marcus Bäumer[a,e]

[a]Institute of Applied and Physical Chemistry, University of Bremen, Germany

[b]Advanced Ceramics, University of Bremen, Germany

[c]Institute for Micro Process Engineering, Karlsruhe Institute of Technology (KIT), Germany

[d]Institute of Inorganic Chemistry and Crystallography, University of Bremen, Germany

[e]MAPEX, Center for Materials and Processes, University of Bremen, Germany

Abstract

Ni and Co containing precursor derived ceramics (ceramers) were prepared from a polysiloxane based preparation route. All catalysts were characterised by BET, XRD and TEM as well as water and heptane adsorption and tested for CO_2-methanation and Fischer-Tropsch synthesis. Different pyrolysis temperature between 400 and 600 °C were used to get catalysts with different surface hydrophilicities. With increasing synthesis temperature less organic groups remain on the surface resulting in a more hydrophilic catalyst. For all Ni containing ceramers, well dispersed particles in the range of 3 nm were formed with comparable surface areas. The catalysts with the lowest tendency towards water adsorption showed the highest activity for CO_2-methanation. From the cobalt containing synthesis route, different material properties were observed. In contrast to the Ni catalysts, the Co particle formation depends on the pyrolysis temperature. While no metallic particles were formed above 400 °C, smallest particles were obtained using a pyrolysis temperature of 500 °C with particle sizes in the range of ~5 nm. With increasing pyrolysis temperature to 600 °C, particle size increases to ~10 nm. Nevertheless, first tests for CO_2-methantion and Fischer-Tropsch reaction were successful and the catalysts with less hydrophilic surface showed higher activity and a higher selectivity towards C_{5+}-products.

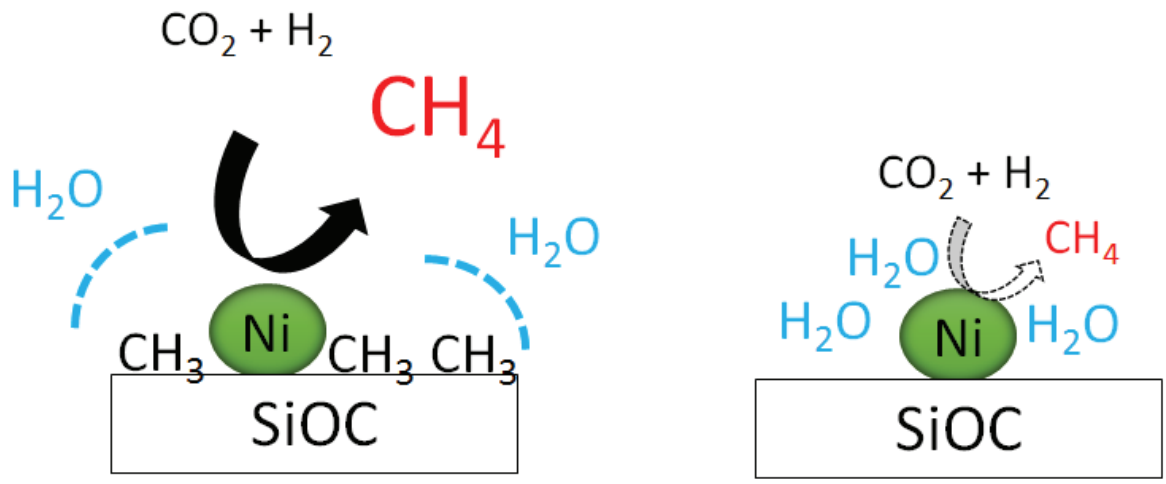

1. Introduction

Co and Ni-catalysts are widely studied catalysts for Fischer-Tropsch synthesis and CO_2-Methanation, which are important catalytic reactions of new energy storage concepts [1] [2]. With the so-called "power-to-gas" (PTG) and "power-to-liquid"-technology (PTL) it is possible to realise the energy supply based on renewable resources in form of heat, electricity and fuel [3]. The PTG technology combines the utilisation of CO_2 with the exploitation of renewable energy [4]. In this case CO_2 is converted with hydrogen, which is obtained by electrolysis using wind or solar energy, into methane with the help of suitable catalysts. Methane can be directly fed to the gas grid or stored in tanks and, when needed, used for heat or electricity production. The Fischer-Tropsch reaction, as part of the PTL technology, converts syngas (a mixture of CO and H_2) to more useful middle distillates [1]. In contrast to fuel from crude oil, the concentration of sulphur is very low, which improves the emission of automobiles and reduces the concentration of undesirable sulphur dioxides [5].

Most investigated catalysts for the CO_2 methanation are Ru-, Rh- and Ni-based catalysts [6] [7] [8] [9] [10] [11] [12] [13] [14] [15]. Rh and Ru are known to be very active for CO_2 methanation at low temperatures, but, due to the high costs of the precious metals, only nickel containing catalysts are nowadays applied in industry [2].

In contrast, supported cobalt catalysts are mainly used in industry for Fischer-Tropsch reaction to produce higher hydrocarbons from syngas. High chain growth probabilities can be achieved at high pressures on cobalt catalysts. Typical conditions are pressures in the range of 1 to 6 MPa and temperatures between 200 °C and 300 °C [16]. Using CO_2 instead of CO, the product yield shifts from higher hydrocarbons to methane [17]. Chakrabarti *et al.* [18] investigated this phenomenon with different CO_2/CO feed gas mixtures on a CoPt-Al_2O_3 catalysts using labeled $^{14}CO_2$. They found that CO_2 is mainly converted into methane, while

CO is converted to higher hydrocarbons, implying two independent reaction pathways for CO and CO_2. Due to this fact, cobalt is also an interesting metal to catalyze the CO_2-methanation. Early studies of Weatherbee and Bartholomew [19] also reported higher intrinsic activities and selectivity for Co/SiO_2 compared to a nickel catalyst supported on SiO_2. In spite of this potential only a few papers focused on cobalt catalysts for CO_2 methanation [20] [21] [22] [23].

For both types of catalysts, the support also has a significant influence on the catalytic activity. The most established supports are SiO_2 and Al_2O_3 with specific surface areas (SSA) between 100 and 500 m^2/g, which offer a high surface area and high dispersion of the active phase [24] [25]. It is known, that Al_2O_3 strongly interacts with Co_3O_4 or NiO forming relatively small crystallites. A main problem of too small particles is the diffusion of the metal phase into alumina and the formation of non-active aluminate spinels [26] [27] [28]. Furthermore, with decreasing particle size the reduction of the metal oxide to the metallic phase becomes more difficult [29]. An enhanced reducibility can be achieved by the addition of noble metals, such as Pt or Pd, at the expense of higher catalysts costs [30]. In contrast, the interaction between metal oxides and SiO_2 is relatively weak, which leads to a better reducibility of the supported metal. At the same time, the dispersion of the metal particles is much lower [1]. Few studies were also carried out on carbon based materials. A good reducibility for cobalt was observed on nanofibers of active carbon for example [31] [32]. Unfortunately due to the weak interaction, sintering of the metal particles under reaction condition occurred.

A relatively new concept is the application of metal based “polymer/precursor derived ceramics” or “ceramers” for heterogeneous catalyzed reactions. In general, polymer or precursor derived ceramics (PDCs) are hybrid materials based on polymers, such as polysiloxane, polycarbosilane, polysilazane or borazine. The preparation route consists of two steps. In a first step, the polymer is crosslinked or gelled. In a second step, the sample is converted into a ceramic material by pyrolysing the sample at high temperatures. To get a material with a high porosity, the samples are converted under a N_2 or Ar atmosphere at temperatures between 400 and 600 °C [33] [34] [35].

PDCs offer many advantages in terms of high thermal stability, low cost, good control of the porosity, composition and simple preparation routes. They are used for many applications, such as filtration, adsorption, membrane separation or sensors [36]. One advantage, in contrast to conventional impregnation method, is the concomitant reduction of the metal during the pyrolysis process. Schmatz *et al.* [37] prepared metal based porous M@SiCN (M =

Fe, Co, Pt, Cu, Ag, Au) from a polysiloxane based route. Metals were reduced *in situ* during the pyrolysis process. For this reason, the separate transformation of the oxide into metallic phase is not necessary and no problems with the formation of spinel or other hard-reducible mixed oxides can occur. Furthermore, PCDs can be used to get a variety of shapes. Foams and monoliths can be prepared by direct foaming or the emulsion approach and also thin coatings can be applied from polysiloxane precursors [38] [39] [40].

Another interesting effect can be achieved by varying the pyrolysis temperature. With increasing temperature, less organic groups stay on the surface, resulting in a more hydrophilic surface and vice versa [41] [42]. The control of the surface hydrophilicity allows the optimization of reactant and product adsorption [43] [44].

It is well known that water is a major product in CO_2-methnanation and Fischer-Tropsch synthesis. Aziz *et al.* [45] studied the effect of water vapor on CO_2-methanation and found a decrease of CO_2 conversion on a Ni based catalyst. The reverse effect can possibly be achieved by the modification of Co-catalyst with organic groups. It was found that the surface hydrophobicity has a positive effect on the FT-activity and selectivity to higher hydrocarbons [46] [47] [48]. Due to organic groups, the catalyst surface hydrophobicity increased and water removal became easier, which results in increasing activity. Moreover, an increasing amount of C_5 - C_{11} products was found. It was hypothesized by Shi *et al.* [48] that the hydrophobic surface leads to prolonged residence time of α-olefins in the pores. It is in general agreement that a higher residence time of α-olefins contributes to re-adsorption on chain growth sites and thus increases the chain growth probability [49].

Only a few studies have been published for metal based PDCs in the field of heterogeneous catalysis in the liquid phase. For example Ni@SiC catalysts were tested for the selective hydrogenolysis of aryl esters and selective hydrogenation of alkynes by Zaheer et al. [50] [51]. Ir based PCDs were prepared and used for the condensation of alcohols [52]. A SiCN ceramic was also used as support for catalytic gas phase reaction. The ceramic sample was impregnated with Pd and additionally tested for the oxidation of methane [53]. A study, where Pt was integrated in a SiC matrix and studied for the oxidation of CH_4 was reported by Kockrick *et al.* [X].The catalyst was prepared from polycarbosilane and a metal containing micro-emulsion before pyrolyzing the sample between 1200 and 1400 °C [54]. In earlier studies of our research group, Adam *et al.* [55] [56] tested Pt containing ceramers for CO oxidation. The preparation route was based on polysiloxane while an additional, complexing agent (Aminopropyl-trithoxysilane) was added to stabilize the metal particles and prevent particle agglomeration on the support. Due to the aminogroups of the aminopropyl-

trithoxysilane (APTES), the metallic ions stabilized during the cross-linking process by complexation. With increasing amounts of APTES, the distribution of the Pt particles was improved, which resulted in increasing activity.

In this study, we used the synthesis route, reported by Adam et al. [55], for the preparation of Ni and Co- based ceramers for CO_2 methanation and Fischer-Tropsch synthesis. The impact of the pyrolysis temperature on the material properties and catalytic activity was studied. To this end, the prepared catalysts were characterized by BET, XRD and TEM. In addition, the surface hydrophilicity was analyzed by water and heptane adsorption measurements.

The purpose was to understand the connection between the variation of the pyrolysis temperature on the material properties and the overall effect on the catalytic activity. Especially, the general effect of the surface hydrophilicity on the CO_2 methanation and Fischer-Tropsch reaction was studied in first experiments.

2.0 Experimental section

2.1 Catalysts preparation:

In a first step, the metal salts $Co(NO_3)_2$ (Alfa Aesar GmbH & Co KG, Cobalt(II)nitrate hexahydrate, ACS, 98.0-102.0%) and $Ni(NO_3)_2$ (Merck KGaA, Nickel(II)-nitrate-hexahydrate), the poly(phenylmethyl)siloxane H44 (Silres® H44, Wacker Chemie AG) and the complexing agent APTES (abcr GmbH, 3-Aminopropyltriethoxysilane, 98%) were separately dissolved in THF. In a second step, the metal precursor solution was slowly mixed with the APTES solution with a ratio of 1:4. The mixed solution was therafter added dropwise to the H44, before adding a 0.2-M-NH_3-solution. The calculated amounts are given in Table 1. The whole solution was stirred at 85 °C for 72 h.

Subsequently, the solvent was removed in a rotating evaporator and the samples dried at 25 °C for 10 h under vacuum. In the following, the samples were cross-linked at 200 °C for 2h. The solid material was milled and pyrolysed at 400, 500 or 600 °C under N_2-atmosphere. The heating rate for the pyrolysis process was 120 °C/h from RT to 100 °C and 30 °C/h to reach the maximum temperature. The maximum temperature was hold for 4 h.

Three Co containing ceramers and three Ni based ceramers were prepared using pyrolysis temperatures of 400, 500 and 600 °C. For comparison also ceramers without any metal were produced. All samples including all preparation details are listed in Table 1.

*Table 1: Materials for preparation, pyrolysis temperature and calculated amount of Co and Ni (*calculated from TG) of prepared ceramers*

Sample	Metal	$n_{Me(NO_3)}$ /mol	polysiloxane n_{H44} /mol	Complexing agent APTES /mol	$\frac{n_{APTES}}{n_{Me(NO_3)_2}}$	Pyrolysis temp. /°C	Metal /wt% after pyrolysis*
Support-400	---	0	1	0.4	---	400	0
Support-500	---	0	1	0.4	---	500	0
Support-600	---	0	1	0.4	---	600	0
30Co-400	Co	0.3	1	1.2	4	400	7.4
30Co-500	Co	0.3	1	1.2	4	500	7.8
30Co-600	Co	0.3	1	1.2	4	600	8.4
30Ni-400	Ni	0.3	1	1.2	4	400	7.4
30Ni-500	Ni	0.3	1	1.2	4	500	7.7

30Ni-600	Ni	0.3	1	1.2	4	600	8.4

2.2 Catalysts characterisation

The specific surface areas were determined by BET (BelSorpMini, BelSorp Inc. Japan) nitrogen adsorption isotherms recorded at 77 K after the samples were outgassed for 12 h at 120 °C under flowing argon.

For the investigation of the surface hydrophilicity and hydrophobicity, water and n-heptane vapour adsorption measurements were conducted at room temperature. In a first step, the weight of the samples was measured after drying at 70 °C. Next, all samples were stored at room temperature for 24h under water or n-heptane vapour atmosphere. After 24h the weight of the samples were measured again and the amount of adsorbate was calculated from the weight difference.

The freshly prepared ceramers were characterized by X-ray diffraction to identify the phases of the metallic compounds and to calculate the average crystallite size of Co and Ni. The samples were analyzed using a Bruker D8 diffracting system. The diffractometer was configured in Bragg-Brentano geometry equipped with a primary Johansson monochromator which provides Cu-$K_{\alpha 1}$ (λ = 0.1540598 nm) radiation. A 0.1° fixed divergence, 4° primary, 2.5° secondary soller slits, and a multi-strip LynxEye detector was used. Scans in the range of 10 – 80° 2θ were applied using a total measurement time of 246 minutes with 4 s per step. In addition the XRD patterns were refined using DiffracPlus Topas 4.2 (Bruker AXS, Karlsruhe, Germany). The background, scale factor, unit cell parameters and peak widths parameters were refined additionally to the Lorentzian crystallite size. For the pattern refinement, the structural models for Ni (ICSD: 41508) with space group $Fm\bar{3}m$ [57] and Co (ICSD: 44989) with space group $Fm\bar{3}m$ [58] were used. The instrumental contribution to the peak broadening was taken into account during the full profile fitting using fundamental parameters derived from a fit of standard crystalline LaB_6.

TEM images were acquired using a Tecnai F20 S-TWIN microscope coupled with an imaging filter. The GATAN imaging filter and a field emission gun were operated at an acceleration voltage of 200 KeV for all measurements. Co and Ni containing ceramers were analysed after different pyrolysis temperatures to get information about the metal distribution and particle size.

2.3 Catalytic tests

The CO_2 methanation reaction was carried out in a quartz U-tube reactor with an inner diameter of 4 mm. For each experiment, 100 mg catalyst (sieve fraction of 100 - 300 µm) and 20 mg SiO_2 (sieve fraction of 100 – 300 µm) were placed in the reactor tube. Before catalytic experiments, the catalyst was activated at 430 °C under flowing hydrogen for 10 h. The temperature was slowly increased from RT to 430 °C with a heating rate of 1 °C /min. The CO_2 methanation reaction was carried out in a temperature range between 200 and 400 °C at atmospheric pressure. The CO_2:H_2 ratio was 1:4 with a total flow rate of 30 mL/min. The measurement time was 30 minutes at each temperature to reach steady state conditions. Each catalyst was tested three times in series. In order to detect the product gases, a compact gas chromatograph (Global Analyser Solution) was used. The GC was equipped with two columns and two TCD detectors. The columns were loaded with two sample tubes in parallel. A molsieve 5Å (15 m, diameter = 0.32 mm) was used for the detection of Ar (internal standard), H_2, CO and CH_4 and a porabond column (15 m, diameter = 0.32mm) was used for analysing Ar (internal standard), H_2 and CH_4 and CO_2.

For the Fischer-Tropsch reaction, a fixed bed reactor was used. A special annular reactor was designed for this purpose to avoid hot spots inside the catalysts bed (bedlength = 107 mm, δ bed = (dbed1 - dbed2)/2 = (15-12)/2 = 1.5 mm). The reactor was equipped with circulating oil for temperature control, which can efficiently remove excess heat. 2 g catalyst was diluted with 6 g SiC to fill up the reactor. First, the reaction products were separated in a 200 ℃ hot trap, where the "wax" was condensed. Then the residual components flowed into a 6 ℃ cold trap, where the "oil" was condensed. At the end, the residual gas was injected into an online GC (Agilent 6890N, equipped with two columns: HP-Plot/Q 19095P-Q04 and HP-Molesieve 19095P-MS6; and two detectors: thermal conductivity detector and flame ionization detector), where the CO and H_2 conversion as well as CH_4 and C_{5+} selectivity could be calculated.

Conversion of a reactant was defined as:

$$x_i = \frac{(\dot{n}_{i,in} - \dot{n}_{i,out})}{\dot{n}_{i,in}} \qquad \text{Eq. 1}$$

where $\dot{n}_i$ is the molar flow rate of component i.

Selectivity of hydrocarbon was defined as:

$$s_i = \frac{\dot{n}_{i,out} \times N_{c,i}}{\dot{n}_{CO,in} - \dot{n}_{CO,out}} \qquad \text{Eq. 2}$$

where $N_{c,i}$ is the carbon number of component i.

Mass fraction of hydrocarbons was defied as:

$$w_i = \frac{m_i}{\sum m_j} \quad \text{Eq. 4}$$

where m_i is the mass of component i in g.

Before starting the measurement, the catalysts were activated at 350 °C for 10 h. The H_2:CO ratio was 1.8 for all tests. The temperature was varied between 220 and 260 °C, while the weight hourly space velocity (WHSV) was 3.1 for the first and 2 g/gKat·h for the second run at each temperature.

3.0 Results and discussion

3.1 Catalyst characterisation

3.1.1 Surface area and water/heptane adsorption

The specific surface area (SSA) was analysed to obtain information about the effect of the pyrolysis temperature on the support porosity. The surface areas of the pure and all metal based ceramers are plotted in Figure 1.

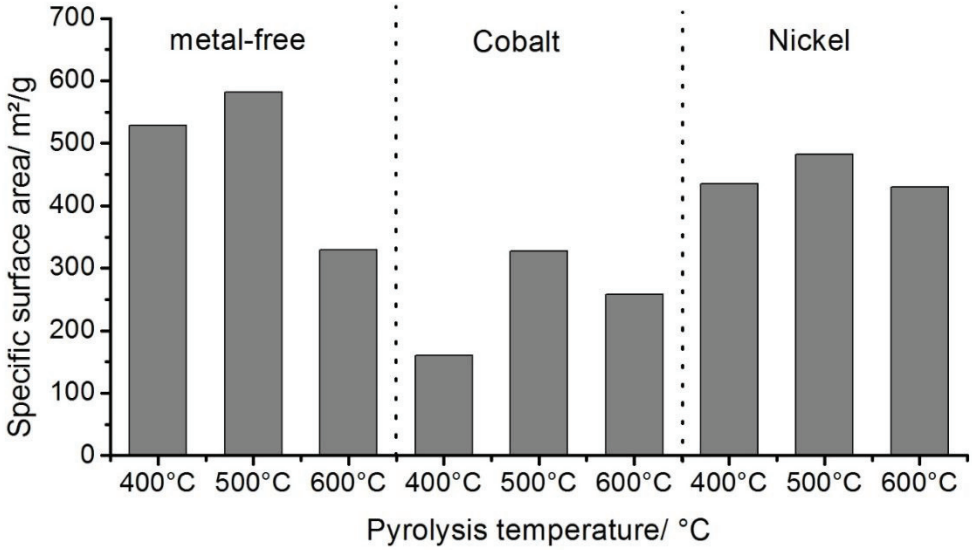

Figure 1: Specific surface are of all prepared Ni, Co and metal free ceramers using different pyrolysis temperatures

Comparing the metal free samples with the Co and Ni containing ceramers, the same overall trend regarding the dependency of the SSA on the pyrolysis temperature was found. With increasing pyrolysis temperature from 400 to 500 °C, the SSA increases. However, further increasing the pyrolysis temperature to 600 °C leads to a decrease of the surface areas again. This behaviour can be explained by the decomposition of the organic material with increasing temperature. The decomposition of the polysiloxane and APTES occurs in a temperature range between 350 and 700 °C [55]. With increasing temperature a higher amount of organic groups are removed resulting in a porous structure. At elevated temperatures, however, the evolved microporosity diminishes again and hence the surface area decreases.

When comparing the absolute SSA values of the three different types of ceramers, a significant difference was found, yet. The highest SSA surface areas are detected for the metal free samples after 400 and 500 °C in the range between 500 and 600 m^2/g, which decreases to around 300 m^2/g at a pyrolysis temperature of 600 °C. The SSAs of the Ni containing

ceramers are in a similar range, but here the difference between the various pyrolysis temperatures is only 50 m²/g. In particular, no drastic decrease of the surface is found upon increasing the pyrolysis temperature to 600°C. The cobalt ceramers show the lowest surface areas of all samples. The catalyst pyrolysed at 400 °C only reaches a value of 160 m²/g. The maximum SSA with ~ 300 m²/g was obtained after pyrolysing at 500 °C. Based on these results, it can be supposed that the metal-APTES complex has an effect on the decomposition of the sample. To get more information about the particle formation and particle size, catalysts were further characterised by XRD and TEM (see *3.1.2* and *3.1.3*).

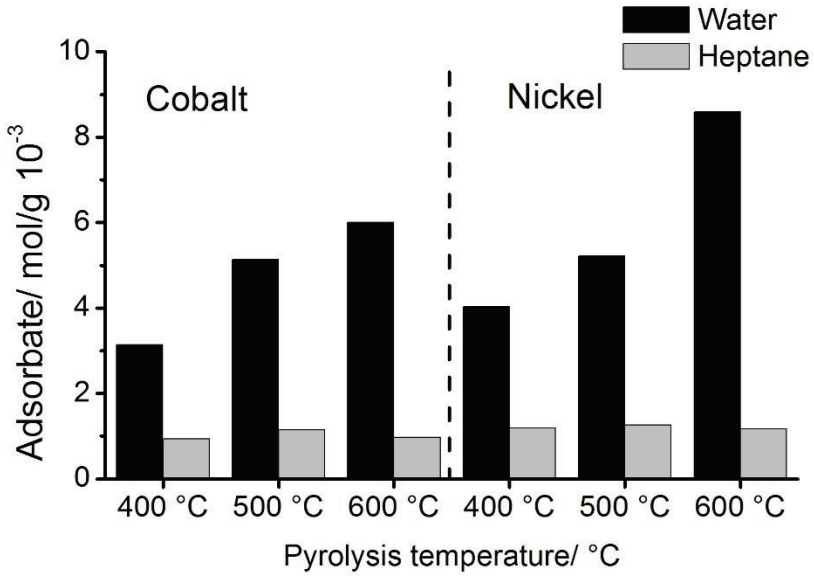

Figure 2: Water and heptane adsorption measurements for Co and Ni based ceramers after different pyrolysis temperatures

The surface hydrophilicity and hydrophobicity depends on the pyrolysis temperature as well. This can be demonstrated by water and heptane adsorption measurements. The results for the Co and Ni ceramers are shown in Figure 2. It is clearly demonstrated that, with increasing pyrolysis temperature, the hydrophilicity of the material increases as well, which is indicated by the increased water adsorption. This is in agreement with earlier studies. With increasing temperature, less hydrophobic organic groups stay on the surface resulting in a more hydrophilic surface [41] [42]. In contrast, the amount of heptane was more or less constant. The low hydrophobicity can be explained by the high APTES/metal ratio, which was used for the synthesis. Adam *et al.* [55] found that an increasing amount of APTES decreases the amount of adsorbed heptane. This can be explained by a higher decomposition of APTES at lower temperatures (~400°C) compared to the polysiloxane. For this reason, the weight loss during the pyrolysis process is much higher for APTES containing samples compared to pure

polysiloxane. Thus, less organic decomposition products are present due to the loss of the aminopropyl groups leaving behind the polar silicon oxide backbone.

3.1.2 XRD

Co and Ni based ceramers and the metal free samples pyrolysed at 500 and 600 °C were analysed by XRD to calculate the average metal crystallite size. The Co containing sample pyrolysed at 400 °C were also characterized to clarify the effect of the low surface area. The diffraction pattern and the refinement results are shown in Figure 3.

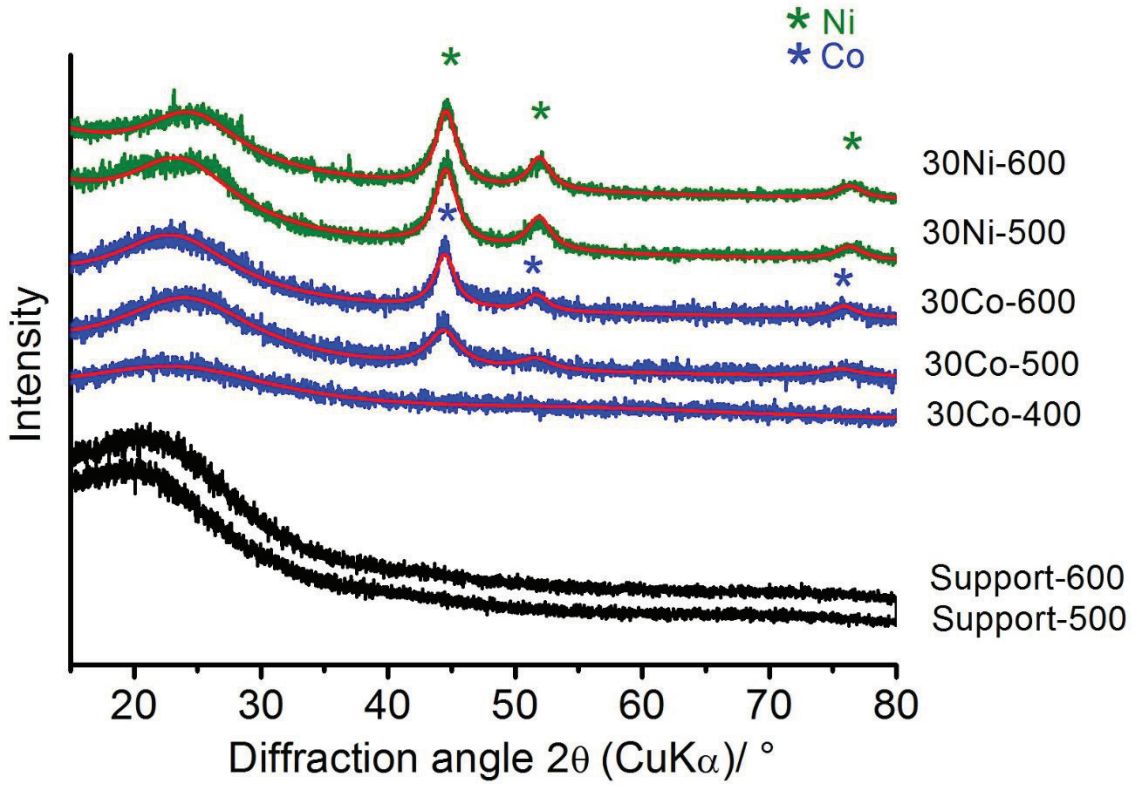

Figure 3: Diffraction patterns of Co (blue), Ni (green) and the metal free ceramers (black) using different pyrolysis temperatures and refined pattern (red).

The metal free samples show only broad reflexions , confirming the formation of a Si based (X-ray) amorphous phase(s). The Co samples pyrolysed at 400 °C are completely amorphous as well. This indicates that the Co complex salt or the Co-APTES complex is still present at 400 °C. In contrast to this, the metal based ceramers pyrolysed at higher temperatures show additional diffraction peaks around 45, 52 and 76° 2θ, indicating the formation of metallic Co and Ni crystallites. To obtain more information about the crystal structures formed, the diffraction patterns were refined using the Rietveld method with the structural models for

cubic metallic Co (space group $Fm\bar{3}m$) and Ni (space group $Fm\bar{3}m$). The calculated diffraction pattern are given by red lines (see Figure 3) showing that all observed reflections can be satisfactorily described. The calculated unit cell parameters and the average crystallite sizes are summarized in Table 2. The lattice parameters were found to be consistent with metallic Co with 357(1) pm as well as metallic Ni with 354(1) pm. The high estimated standard deviations found for the lattice parameters are caused by the small average crystallite sizes of the phases. The smallest crystallite size was found for the Co sample pyrolysed at 500 °C with 2.0(1) nm. With increasing pyrolysis temperature to 600 °C the crystallite size increases to 3.1(1) nm. For the Ni based ceramers a crystallite size of 2.9(1) nm was found, independent of the preparation temperature.

Table 2: Cell parameter, average crystallite size calculated from XRD and average particle size obtained from TEM for Co and Ni based ceramers

Catalyst name	**Lattice parameter a /pm**	**Average Crystallite size /nm XRD**	**Average Particle size /nm TEM**	**Average crystallites/ particle**
30Co-400	No Cobalt	No Cobalt	---	---
30Co-500	357(1)	2.0(1)	5.7	2.8
30Co-600	356(1)	3.1(1)	10.2	3.3
30Ni-400	-	-	3.1	-
30Ni-500	353(1)	2.9(1)	3.2	1.1
30Ni-600	354(1)	2.9(1)	3.5	1.2

3.1.3 TEM

TEM images of all Co and Ni based ceramers – pyrolysed at 400, 500 and 600 °C - and the ceramers pyrolysed at 500 °C after catalysis are shown in Figure 4 a-h.

Comparing Figure 4 a to c of the freshly prepared Co ceramers, the effect of the pyrolysis temperature is clearly demonstrated. Using a pyrolysis temperature of 400 °C, no Co particles are discernible, which is in agreement with XRD pattern shown in Figure 3. In comparison to this, homogenously distributed Co particles are formed using a pyrolysis temperature of 500 °C. By further increasing the pyrolysis temperature to 600 °C a strong increase of the Co particle size is found. The average particle size were calculated from TEM figures using 200

particles and are listed in Table 2. Apparently, the crystallite size, calculated from XRD differs from the particle size calculated from TEM, namely the particle size of Co were 3 time higher as derived from the TEM data as compared to XRD (Table 2), which is evidence for the formation of Co agglomerates consisting of several Co crystallites. Nevertheless, no sintering of the Co particles was found after catalytic reaction (see Figure 4 a and d).

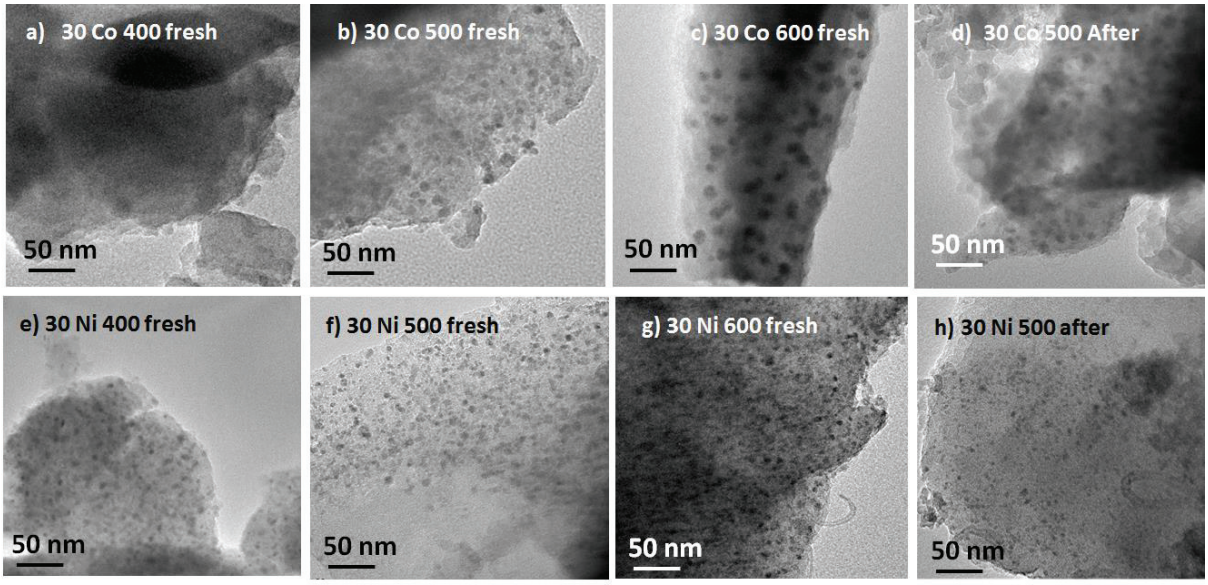

Figure 4: TEM images of fresh prepared Co and Ni based ceramers after pyrolysis at 400, 500 and 600 °C (a-c and e-g) and the 30Ni sample pyrolysed at 500 °C after catalytic measurement (d+h)

In contrast to the Co containing catalysts, the metal dispersion of Ni ceramers is very high, regardless of the pyrolysis temperature (Figure 4 e-g). In addition, the average particle size determined from TEM data is almost the same as the average crystallite size calculated from XRD pattern, indicating the formation of single crystalline Ni particles. In addition, the Ni particle size is stable under reaction conditions, as inferable from figure 4h.

Clearly, BET, XRD and TEM investigations suggest that there is a difference if ceramers are prepared with Co or Ni. In summary, 3 nm Ni particles are formed in all ceramers, independent of the pyrolysis temperature. In contrast, metallic Co particles can only be formed using higher pyrolysis temperatures of 500 and 600 °C. Furthermore, the size of the Co-particles is slightly higher and increases with increasing pyrolysis temperature form ~5 nm to ~10 nm. Why the tendency of particle agglomeration is slightly higher for Co is still unclear.

3.2 Catalytic tests

3.2.1 CO_2-Methanation on Ni ceramers

The XRD, TEM and BET measurements revealed that all Ni based ceramers pyrolysed between 400 and 600 °C show comparable surface areas with homogeneously distributed Ni particles around 3 nm. The only difference was found to be the hydrophilicity, as shown by the water adsorption measurements. With increasing pyrolysis temperature, the surface is more hydrophilic. All three samples were tested for CO_2 methanation between 250 and 400 °C. For each temperature the steady state conversion was reached after a few minutes. Three runs in total were carried out to get information about the stability of the catalysts under reaction condition. Due to the fact, that the conversion levels of the second and third run did not differ from each other, the results of the first and the last run are shown in Figure 5.

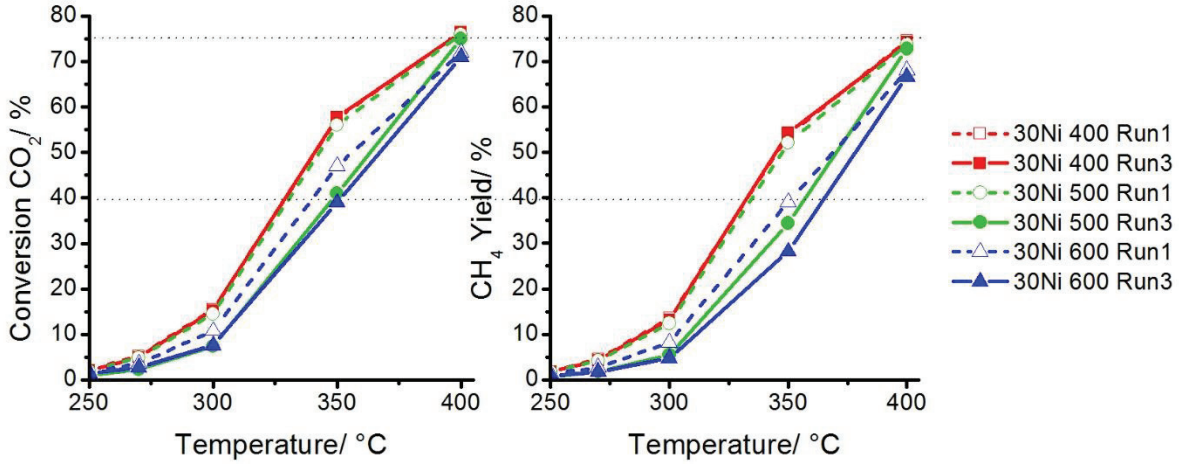

Figure 5: CO_2-methanation (left) and CH_4 yields (right) for Ni ceramers, pyrolysed at 400, 500 and 600 °C

It is clearly shown that the CO_2 conversion increases with increasing temperature for all samples. The highest activity can be observed for the catalysts with the lowest tendency to adsorb water, i.e. the sample pyrolysed at 400°C. Interestingly no deactivation was found for this catalyst after the first run. In contrast, the catalysts pyrolysed at higher temperatures lost around 20 to 30% activity after the first run. The same trend was also found for the CH_4 yield. The main product was CH_4 for all samples, but also a low amount of CO was detected. This amount of CO was slightly higher for the catalysts with a more hydrophilic surface.

From these results it can be concluded, that the surface hydrophilicity has an effect on the CO_2 methanation. It is known, that the product water has an inhibiting effect on the methanation activity [45]. During the reaction, adsorbed water hinder the accessibility of the active sites. For this reason, the conversion rate decreases. It can be supposed that this effect can be diminished using a catalysts with a less hydrophilic surface. Less water is adsorbed on the surface and the amount of blocked active sites can be reduced.

The next step to further improve the activity would be the optimisation of the APTES/metal ratio for the preparation of a more hydrophobic surface without losing the stability of the Ni particles on the support.

3.2.2 CO_2-Methanation and Fischer-Tropsch on Co-ceramers

In the case of the Co containing ceramers, XRD, BET and TEM investigations indicated that the pyrolysis temperature has a significant effect on the average crystallite and particle size, surface area and particle size distribution. No particles are formed after pyrolysis at 400 °C, while small and homogenous Co particles are formed using a pyrolysis temperature of 500 °C. At higher pyrolysis temperatures (600 °C) larger polycrystalline particles form.

Due to the agglomeration of the particles, a lower metal surface is available on the catalysts pyrolsed at 600 °C. Although the CO_2 conversion rate is slightly lower, CO_2 methanation activity, which is shown in Figure 6 follows the same trend.

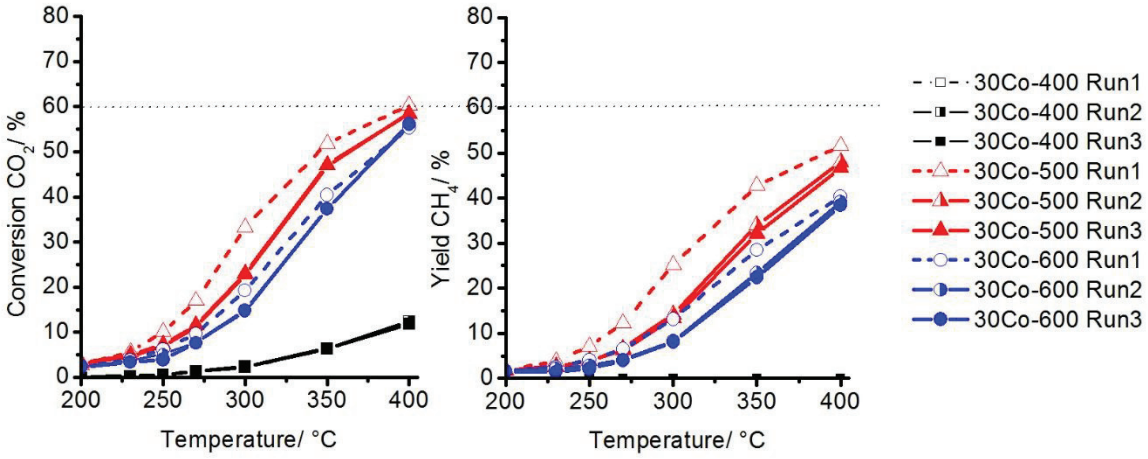

Figure 6: CO_2-methanation (left) and CH_4 yields (right) for Co ceramers, pyrolysed at 400, 500 and 600°C.

The Co creamer, pyrolysed at 400 °C, shows no activity for CO_2-methanation. Only CO was detected between 300 and 400 °C, indicating a low activity for the reverse water gas shift (RWGS) reaction. The other two ceramers show a moderate activity and CH_4 yield, while the

activity was higher for the Co sample with smaller Co particles. Due to different particle sizes, it is not possible to clearly clarify the impact of the surface hydrophilicity.

Nevertheless, to study the effect of the surface hydrophilicity, Fischer-Tropsch reaction was carried out for the Co ceramers pyrolysed at 500 and 600 °C. It is known that a more hydrophobic surface can increase the chain growth probability due to a higher residence time of α-olefines inside the pores [48]. Moreover, the particle size has also a huge effect on the selectivity. The smaller the particle size the lower the chain growth probability [59]. Bezemer *et al.* [32] studied the effect of the cobalt particle size on inert carbon nanofibers in the range of 2.6 to 27 nm for the FT-Synthesis. With decreasing particle size from 16 to 2.6 nm, the TOF decreased from $23 \cdot 10^{-3}$ to $1.4 \cdot 10^{-3}$, while C_{5+} selectivity decreased from 85 to 51 wt% at 3.5 MPa. The authors conclude that the required cobalt particle size for efficient FT is larger than 6-8 nm.

In our case, the catalyst pyrolysed at 600 °C has a particle size around 10 nm, demonstrated by TEM, while the particle size for the 500 °C pyrolysed sample is much smaller (~ 3 nm). On the other side, the hydrophilicity is higher for the catalyst with larger particles. The CO conversion and selectivity for both samples are summarized in Table 3.

Table 3: Fischer-Tropsch reaction of Co500 and Co600 between 220 and 260 °C at 2 MPa

Catalyst	Temp. /°C	WHSV/ /g/gKat·h	CTY · 10^{-4} /molCO/gKat·s	CO /%	CH_4 /%	C_2-C_4 /%	C_{5+} /%	$\frac{O_{C_2-C_4}}{P_{C_2-C_6}}$
Co500	220	3.1	13.8	7.1	74.9	15.4	9.7	0.16
Co500	220	2.0	19.7	10.1	65.3	13.6	21.2	0.23
Co500	240	3.1	32.1	16.5	59.0	13.2	27.8	0.25
Co500	240	2.0	43.9	22.5	52.3	8.3	39.4	0.13
Co600	220	2.0	<10	<5	mainly	Low	Low	low
Co600	240	3.1	16.7	8.6	88.5	11.1	0.4	0.13
Co600	240	2.0	23.0	11.8	77.6	10.9	11.5	0.18
Co600	260	3.1	30.6	15.7	74.5	10.9	14.6	0.28
Co600	260	2.0	41.1	21.1	65.5	9.8	24.7	0.34

The sample, pyrolysed at 500 °C shows much higher activities and also a higher C_{5+} yield as compared to the Co ceramers pyrolysed at 600 °C. Around 20 °C higher temperature was necessary for the sample pyrolysed at 600 °C to reach the same FTS activity. Furthermore,

comparing the selectivity at comparable CTYs, the catalysts pyrolysed at 500 °C resulted in C_{5+} selectivity which is around 10-15% higher. As explained above, an improved FT-performance can be achieved with increasing Co-catalysts particles size and decreasing hydrophilicity. In our case, the sample pyrolysed at 600 °C has the biggest particle size and the other sample (pyrolysed at 500 °C) has the lowest hydrophilicity. In spite of a much lower particles size, the sample (pyrolysed at 500 °) with a lower surface hydrophilicity gives rise to the better FT-performance. From this we can conclude that the impact of the surface hydrophilicity dominates. For the investigated Co-catalysts, the C_{5+}-selectivity is until now not comparable with industrial chain growth probabilities, but the selectivity can be further enhanced if it is possible to other precursor salt (like Co-acetate or Co-chloride) and less APTES to increase the particles size and hydrophobicity in parallel.

4.0 Conclusion

Co and Ni ceramers were prepared using three different pyrolysis temperatures between 400 and 600 °C. For all prepared samples, an increasing surface hydrophilicity was found with increasing pyrolysis temperature, due to less organic groups on the surface. All Ni catalysts showed well distributed Ni particles in the range of 3 nm and high surfaces areas around 450 m^2/g, as demonstrated by TEM, XRD and BET investigations. The three different Ni catalysts were tested for CO_2-methanation and it was found that a lower hydrophilicity has an enhancing effect on the activity. It can be supposed that the inhibition of active sites due to adsorbed water can be lowered with decreasing surface hydrophilicity.

Using cobalt for the synthesis of ceramers, material properties differ from Ni ceramers. After 400 °C, no metallic particles are formed. But increasing the pyrolysis temperature to 500 °C leads to the formation of well distributed particles in the range of 3 nm. Using the highest pyrolysis temperature of 600 °C, larger Co agglomerates in the range of 10 nm were formed. Due to the higher metal dispersion, the 500 °C pyrolysed sample showed the highest activity for CO_2 methanation. A lower activity was found for the sample pyrolysed at 600 °C, while the sample prepared with the lowest pyrolysis temperature showed no activity for CO_2-methantion. In first experiments, the two active Co catalysts were tested for Fischer-Tropsch synthesis to investigate the influence of the hydrophilicity. The sample with the lowest hydrophilicity showed the best FT-performance in spite of the fact that the particles were by a factor of around 3 smaller as compared to creamers pyrolysed at higher temperatures resulting in more hydrophilic surfaces.

In summary, we could demonstrate that the metal based ceramers prepared from polysiloxanes are promising catalysts with tuneable surface properties. Especially for catalytic reactions, where water has a negative influence on activity or selectivity, improved activities and enhanced selectivities can be achieved.

Acknowledgements:

This work was part of the Research Training Group GRK 1860 “Micro-, meso- and macroporous nonmetallic Materials: Fundamentals and Applications” (MIMENIMA) and we grateful thanks the German Research Foundation (DFG) for financial support.

Keywords:

CO_2-methanation, Fischer-Tropsch, Nickel catalysts, Cobalt catalyst, Precursor derived ceramic, surface hydrophilicity

Literature:

[1] A. Y. Khodakov, W. Chu und P. Fong, *Chem. Rev. 107,* pp. 1692-1744, 2007.

[2] W. Wang und J. Gong, *Front. Chem. Sci. Eng. 5,* pp. 2-10, 2011.

[3] K. Purr, D. Osiek, M. Lange und K. Adlu, „www.umweltbundesamt.de," 2016. [Online]. Available: http://www.umweltbundesamt.de/publikationen/integration-von-power-to-gaspower-to-liquid-in-den. [Zugriff am 2016].

[4] T. Riedel, *App. Catal. A 186,* p. 201, 1999.

[5] A. Jess und P. Wasserscheid, *UWSF- Z Umweltchem. Ökotox. 14,* pp. 145-154, 2002.

[6] A. Beulsa, C. Swalusa, M. Jacquemina, G. Heyenb, A. Karelovica und P. Ruiza, *Appl. Catal. B 113,* pp. 2-10, 2012.

[7] L. Bian, L. Zhang, R. Xia und Z. Li, *J. Nat. Gas. Sci. Eng. 27,* pp. 1189-1194, 2015.

[8] M. Ding, J. T. Tu, Q. Zhang und M. Wang, *Biomass Bioenerg. 85,* pp. 12-17.

[9] G. Du, S. Lima, Y. Yangb, C. Wanga, L. Pfefferlea und G. L. Hallera, *J. Catal. 249,* pp. 370-379, 2007.

[10] M. S. Duyar, A. Ramachandran und C. Wan, *Journal of CO2 Utilization 12,* pp. 27-33, 2015.

[11] Z. Fan, K. Sun, N. Rui, B. Zhao und C.-j. Liu, *J. Energy Chem. 24,* pp. 655-659, 2015.

[12] M. Kuśmierz, *Catal. Today 137,* pp. 429 - 432, 2008.

[13] C. K. Vance und C. H. Bartholomew, *Appl. Catal. 7,* pp. 169 - 177, 1983.

[14] G. D. Weatherbee und C. H. Bartholomew, *J. Catal. 68,* pp. 67-76, 1981.

[15] A. Zamani, R. Ali und W. Abu Bakar, *J. Ind. Eng. Chem. 29,* pp. 238-248.

[16] G. van der Laan und A. Beenackers, *Catal. Rev. 41,* pp. 255-318, 1999.

[17] Y. Yao, X. Liu, D. Hildebrandt and D. Glasser, *Chem. Eng. J. 193-194,* pp. 318-327, 2012.

[18] D. Chakrabarti, A. de Klerk, V. Prasad, M. K. Gnanamani, W. D. Shafer, G. Jacobs, D. E. Sparks and B. H. Davis, *Ind. Eng. Chem. Res. 54,* pp. 1189-1196, 2015.

[19] G. D. Weatherbee and C. H. Bartholomew, *J. Catal. 87,* pp. 352-362, 1984.

[20] W. A. W. A. Baker, R. Ali, A. A. A. Kadir, S. J. M. Rosid und N. S. Mohammad, *Journal of Fuel Chemistry and Technology 40,* pp. 822-830, 2012.

[21] J. Janlamool, P. Praserthdam und B. Jongsomjit, *J. Nat. Gas. Chem. 20,* pp. 558-564, 2011.

[22] N. Srisawad, W. Chaitree, O. Mekasuwandumrong, A. Shotipruk, B. Jongsomjit and J. Panpranot, *Reac. Kinet. Mech. Cat. 107,* pp. 179-188, 2012.

[23] G. Zhou, T. Wu, H. Xie und X. Zheng, *Int. J. Hydrogen Energy 38,* pp. 10012-10018, 2013.

[24] C.-P. Huang und W. Stumm, *Surf. Sci. 32,* pp. 287-296, 1972.

[25] X. Yan, Y. Liu, B. Zhao, Z. Wang, Y. Wang und C.-j. Liu, *Int. J. Hydrogen Energ. 38 ,* pp. 2283-2291, 2013.

[26] R. L. Chin und D. M. Hercules, *J. Phys. Chem. 86,* pp. 360-367, 1982.

[27] W. J. Wang und Y. W. Chen, *Appl. Catal. 77,* pp. 223-233, 1991.

[28] O.-S. Joo und K.-D. Jung, *Bull. Korean Chem. Soc. 23,* pp. 1149-1153, 2002.

[29] G. Prieto, A. Martínez, P. Concepción and R. Moreno-Tost, *J. Catal. 266,* pp. 129-144, 2009.

[30] M. de Beer, A. Kunene, D. Nabaho, M. Claeys und E. van Steen, *The Journal of The Southern African Institute of Mining and Metallurgy 114,* pp. 157-165, 2014.

[31] H. Zhang, W. Chu, C. Zou, Z. Huang, Z. Ye und L. Zhu, *Catal. Lett. 141,* pp. 438-444, 2011.

[32] G. Bezemer, J. H. Bitter, H. P. C. E. Kuipers, H. Oosterbeek, J. E. Holewijn, X. Xu, F. Kapteijn, A. J. van Dillen und K. P. de Jong, *J. Am. Chem. Soc. 128 ,* p. 3956, 2006.

[33] V. Gualandris, D. Hourlier-Bahloul und F. Babonneau, *J. Sol-Gel Technol. 14,* pp. 39-48, 1999.

[34] P. Mutin, *J. Sol-Gel Sci. Technol. 14,* pp. 27-38, 1999.

[35] H. Schmidt, D. Koch und G. Grathwohl, *Chem. Eng. Technol. 23,* pp. 959-964, 2000.

[36] C. Vakifahmetoglu, D. Zeydanli und P. Colombo, *Mat. Sci. Eng. R 106,* pp. 1-30, 2016.

[37] T. Schmalz, T. Kraus, M. Günthner, C. Liebscher, U. Glatzel, R. Kempe und G. Motz, *Carbon 49,* pp. 3065-3072, 2011.

[38] M. Adam, S. Kocanis, T. Fey, M. Wilhelm and G. Grathwohl, *J. Eur. Ceram. So. 34,* pp. 1715-1725, 2014.

[39] M. Adam, C. Vakifahmetoglu, P. Colombo, M. Wilhelm and G. Grathwohl, *J. Am. Ceram. Soc. 97,* pp. 959-966, 2014.

[40] F. Schlüter, J. Meyer, M. Wilhelm und K. Rezwan, *Colloids Surf. A 492,* pp. 160-169.

[41] T. Prenzel, M. Wilhelm und K. Rezwan, *Microporous Mesoporous Mater. 169,* pp. 160-167, 2013.

[42] M. Wilhelm, M. Adam, M. Bäumer und G. Grathwohl, *Adv. Eng. Mater. 10,* pp. 241-245, 2008.

[43] T. Blasco, M. Comblor, A. Corma, P. Esteve, J. Guil und A. Martinez, *J. Phys. Chem. B 102,* pp. 75-88, 1998.

[44] M. Camblor, A. Corma, P. Esteve, A. Martinez und S. Valencia, *Chem. Commun. 8,* pp. 795-796,

1997.

[45] M. A. A. Aziz, A. A. Jalil, S. Triwahyono and M. W. A. Saad, *Chem. Eng. J. 260,* pp. 757-764, 2015.

[46] R. Xie, D. Li, B. Hou, J. Wang, L. Jia und Y. Sun, *Catal. Comm. 12,* pp. 589-592, 2011.

[47] L. Jia, L. Jia, D. Li, B. Hou, J. Wang und Y. Sun, *J. Solid State Chem. 184,* pp. 488-493, 2011.

[48] L. Shi, J. Chen, K. Fang und Y. Sun, *Fuel 87,* pp. 521-526, 2008.

[49] E. Iglesia, S. Reyes, R. Madon und S. Soled, *Adv. Catal. 39,* pp. 221-302, 1993.

[50] M. Zaheer, J. Hermannsdorfer, W. Kretschmer, G. Motz und R. Kempe, *Chem. Cat. Chem. 6,* pp. 91-95, 2014.

[51] M. Zaheer, C. D. Keenan, J. Hermannsdörfer, E. Roessler, G. Motz, J. Senker und R. Kempe, *Chem. Mater. 24,* pp. 3952-3963, 2012.

[52] D. Forberg, J. Obenauf, M. Friedrich, S. Huhne, W. Mader, G. Motz und R. Kempe, *Catal. Sci. Technol. 4,* pp. 4188-4192, 2014.

[53] S. Schwarz, M. Friedrich, G. Motz und R. Kempe, *Z. Anorg. Allg. Chem. 641 ,* pp. 2266-2271, 2015.

[54] E. Kockrick, R. Frind, M. Rose, U. Petasch, W. Böhlmann, D. Geiger, M. Herrmann and S. Kaskel, *J. Mater. Chem. 19,* pp. 1543-1553, 2009.

[55] M. Adam, M. Wilhelm and G. Grathwohl, *Microporous and Mesoporous Materials 151,* pp. 195-200, 2012.

[56] P. Sonström, M. Adam, X. Wang, M. Wilhelm, G. Grathwohl and M. Bäumer, *J. Phys. Chem. C 114,* pp. 14224-14232, 2010.

[57] J. Haglund , F. Fernandez Guillermet und G. Grimvall, *Physical Review B 48,* pp. 11685-11691, 1993.

[58] E. Owen und D. Madoc Jones, *Proceedings of the Physical Society 67,* pp. 456-466, 1954.

[59] N. Fischer, E. van Steen und M. Claeys, *J. Catal. 299,* pp. 67-80, 2013.

[60] U. Jeong and y. Kim, *J. Ind. Eng. Chem. 31,* pp. 393-396, 2015.